Regional Studies in Marine Science 45 (2021) 101834

Contents lists available at ScienceDirect

Regional Studies in Marine Science

journal homepage: www.elsevier.com/locate/rsma

Geochemical mapping of a blue carbon zone: Investigation of the influence of riverine input on tidal affected zones in Bull Island

Anthony Grey [a], Aisling Cunningham [a], Alan Lee [a], Xavier Monteys [b], Seamus Coveney [a], Margaret V. McCaul [c], Brian T. Murphy [d], Thomas McCloughlin [e], Brooks Hidaka [f], Brian P. Kelleher [a,*]

[a] School of Chemical Science. Dublin City University, Ireland
[b] Geological Survey of Ireland, Ireland
[c] Insight SFI research Centre for Data Analytics, Dublin City University, Ireland
[d] Enrich Environmental Ltd, Ireland
[e] School of STEM Education, Innovation and Global Studies, DCU Institute of Education, Dublin City University, Ireland
[f] Department of Chemistry, The University of Kansas Lawrence, KS 66045, United States of America

ARTICLE INFO

Article history:
Received 2 October 2020
Received in revised form 8 April 2021
Accepted 7 May 2021
Available online 8 May 2021

Keywords:
Blue carbon
Coastal spit
Geochemical mapping
Artificially constructed wetlands
Mudflats
Salt marshes
Polyaromatic hydrocarbons
Anthropogenic impacts

ABSTRACT

Bull Island (BI) is a coastal sand spit that formed as an unintended consequence of the construction of two walls, built over 200 years ago in Dublin Port, Ireland to alleviate silting of the shipping route. A large lagoon, on the land side of the island was separated in 1964 by the construction of a causeway to produce two separate lagoons that are now impacted by different water sources. Here we investigate the influence of riverine inputs on the two adjacent but unconnected tidal wetland lagoons. The South lagoon (SL) is supplied by tidal water passing through the eutrophic R. Liffey and R. Tolka estuary zones, while the North Lagoon (NL) is supplied by seawater and to a lesser degree, freshwater from the R. Liffey plume. Within each of these zones a clear ecotone exists between the mudflats (MF) and vegetated saltmarshes (SM). We determined the quantity and distributions of bulk geochemical characteristics across BI's sediments, including total organic carbon (TOC), total nitrogen (TN), metals, and also, 16 individual polyromantic hydrocarbon's (PAH's) as an indication of anthropogenic input. Primary focus was placed on studying the blue carbon sediments of the lagoon zones. Significant differences in analytical results showed major influences exerted on sediment geochemistry within each lagoon. This study highlights the ability of a functioning coastal wetland to flourish and sequester elevated levels of carbon, metals and pollutants under the constraints of increasing anthropogenic impact. As the inadvertent result of geo-engineering, BI and its environs is a very important site to investigate the potential of artificially constructed wetlands to act as blue carbon reservoirs.

1. Introduction

The effects of climate change have already been seen globally (AR5 climate change, 0000), with predictions of higher rainfall and an increase in storms modelled for Ireland in the future (Dwyer, 2012). Coastal wetlands are known sinks for carbon and can continue to act to mitigate climate change even as sea levels rise (Rogers et al., 2019). They provide a myriad of wildlife habitats (Sutton-Grier and Sandifer, 2018) and help to protect coastal communities and economies by functioning as natural sponges that can lower flood heights (Schuerch et al., 2018; Narayan et al., 2017) and dissipate storm surges (Gedan et al., 2011), protect against erosion (Costanza et al., 2008), capture of metals and pollutants, and cycling of nutrients (Renzi et al., 2019).

In recent years, scientists and policymakers have pushed to highlight and protect carbon stored in coastal wetlands, known as *blue carbon* (Tollefson, 2018). Blue carbon is the term for carbon sequestered by the world's ocean and coastal ecosystems. Tidal wetlands and vegetated coastal marshes have a very high capacity for the uptake and long-term storage of carbon (Kelleway et al., 2017). The high capacity for carbon storage is a result of at least three characteristics of coastal wetlands: (1.) They can efficiently capture and assimilate particulate carbon originating from within the ecosystem and/or from external sources (Kennedy et al., 2010), (2.) Halophytic plants growing in these environments are very productive in converting CO_2 into plant biomass (Nixon, 1980; Alongi, 2002) and (3.) The biogeochemical conditions within sediments lock carbon in by slowing

* Corresponding author.
E-mail address: brian.kelleher@dcu.ie (B.P. Kelleher).

https://doi.org/10.1016/j.rsma.2021.101834

the decay of organic material (Fourqurean et al., 2012; Kristensen et al., 2008; McLeod et al., 2011).

Blue carbon zones existence at the interface between terrestrial, riverine, estuarine, and marine ecosystems, means these sediments receive considerable waterborne allochthonous and anthropogenic inputs from different sources. The convergence of fluvial organic matter, sediments, and pollutants within these waters results in the inevitable deposition of substrates and sediment accretion where hydrological energy dissipates (Fagherazzi, 2013; Cott et al., 2018). The evolution of coastal wetlands provides additional valuable ecosystem services through capture of elevated anthropogenic inputs of metals such as Pb and Zn, nutrients (N and P) and pollutants from both nearby urbanised coastal zones and terrestrially derived sources (Doyle and Otte, 1997; Merrill and Cornwell, 2000; Liu et al., 2017). One such class of pollutants is polycyclic aromatic hydrocarbons (PAHs) that have been extensively studied due to their toxic, mutagenic, and carcinogenic effects (Cachot et al., 2006; Kim et al., 2013; Vane et al., 2007). Anthropogenic PAH sources include combustion of fossil fuels, vehicle emissions, petrochemical spills and burning of biomass (Long et al., 1995). A knowledge of PAH concentrations in coastal and oceanic sediments is helpful for the evaluation of ecosystem health due to their bio accumulative potential, while also providing a useful proxy for the measurement of human impact on sediments. The innate ability of natural wetlands to treat metal contaminated surface water (phytostabilization), remediate sites with elevated sediment PAHs (phytoremediation) and remove excess nutrients from water bodies is widely known and exploited through the use of constructed wetlands (Loomis and Craft, 2010; Vymazal, 2007, 2011; Stumpner et al., 2018). Ultimately, C and associated sediment constituents in such settings can accumulate for centuries but will be very much influenced by processes such as sea-level change, ocean acidification, increased flooding, periods of drought and anthropogenic contributions (Castillo et al., 2000). Future restoration, coastal protection and carbon sequestration schemes will need to consider coastal sediment characteristics and their potential to capture, cycle and sequester both marine and terrestrial derived materials. A model site which will help in this regard is Bull Island (BI), a functioning coastal filter in Dublin Bay, Ireland.

BI (53.3705° N, 6.1440° W) is a coastal sand spit expanding 5 km north-eastwards from the north wall of Dublin Port and 800 m in breadth at its widest point. It formed as an unintended consequence of the construction of north and south Bull walls, built over 200 years ago in Dublin Port, to alleviate silting of the shipping route. Tidal changes induced by the construction of the walls resulted in the deposition of sand and silt in North BI and an actively accreting dune system that continues to this day (National parks & wildlife service, 0000). The growth of the island in the nineteenth century resulted in a sheltered, single shallow creek or lagoon between the island and the mainland (O'Reilly and Pantin, 1956). Sheltered lagoon zones provide an area of energy dissipation for incoming tidal water, thus facilitating higher levels of deposition for suspended particles. Tidal waters from the two ends of the island met between the Naniken Brook and Santry river (Fig. 1). During this time approximately 200 metres' breadth of vegetated saltmarsh emerged, driven by silt deposition coming mainly from the river Liffey (Brooks et al., 2016). In 1964, the area where the tides met in the lagoon was used to build a causeway to make the northern part of the island more accessible. This had the effect of making two independent lagoons, north lagoon (NL) and south lagoon (SL), zones analogous to artificially constructed wetlands, each with their own characteristics. The lagoons are fed by different freshwater and tidal sources (Fig. 2a and Fig. SI.12 A and B), with the SL directly connected to the Tolka estuary, while the NL receives mixed waters passing into Sutton creek through the R. Liffey plume. BI's tidal wetland zones shares the capability of coastal wetlands to sequester carbon (blue carbon), immobilise and treat anthropogenic and natural contamination, create wildlife habitats and provide protection from sea-level rise (SLR) and storms.

Nutrient input into the BI lagoons has been a major problem in the past, with the main sources including input from rivers (Wilson, 2005), raw sewage and industrial pollution (Murphy et al., 2016; Skerrett and Holland, 2000; O'Sullivan, 2019; Wilson et al., 1986; O'Higgins and Wilson, 2005). BI is adjacent to Dublin Port (Fig. 1), the busiest port in Ireland, which contains several other industries including a wastewater treatment plant and a waste-to-energy incinerator. The Bull lagoons have consistently been identified as the areas that have been most impacted by pollution (Jeffrey et al., 1978a; Wilson et al., 1986). Particulates from sewage and rivers have been identified as a major reason for both the productivity and the structuring of the food web in Dublin Bay, and are a major influence of the energy budget for the bay (Wilson et al., 2002; Wilson and Parkes, 1998).

To the best of our knowledge this is the first study to recognise BI's lagoon sediments as a functioning blue carbon ecosystem. We investigate sediment geochemistry in an understudied area of Dublin Bay and provide information on the storage of OM, bulk sediment chemistries and anthropogenic contaminants (i.e. PAHs, Pb and Zn) across BI. Additionally, we specifically focus our discussion of results on BI's tidal lagoon zones to explore the distributions of bulk sediment characteristics (%OC, TN, %clay and silt), metal and PAH accumulation in two adjacent but unconnected tidal wetlands. It was expected that vegetated sediments should accumulate higher carbon, metals and PAH concentrations than non-vegetated sediments due to the trapping effect of above ground biomass, and higher elevation that facilitates more efficient particle deposition. We also hypothesised that higher accumulations would also occur in the SL when compared to the NL due to proximity to the R. Liffey and R. Tolka estuaries where higher riverine transport of anthropogenic materials and higher algal biomass would result in increased concentrations of OM, metals and PAH's. Therefore, the aims of the study were as follows:

- To measure, map and report sediment properties for 59 sample locations covering representative zones across all of BI.
- To measure and assess the differences in the bulk geochemical characteristics (OC, TN, metals), PAHs and other sediment parameters (pH, EC and SOM) between vegetated (Saltmarsh) and un-vegetated (Mudflats) wetland sediments across two tidal lagoons.
- To determine differences in sediment properties (including C accumulation, metal and PAH distributions) between the SL connected to an estuarine system and the NL receiving waters with higher marine mixing.

The overall study provides a baseline record of sediment geochemistry and the influence of urbanisation on a coastal ecosystem in a highly productive blue carbon area.

1.1. Study area

The formation and continual advancing of BI (53.3705° N, 6.1440° W) involves a combination of constant destruction and growth, dictated by the hydrological dynamics of Dublin Bay. Tidal flow in the bay moves from a south to north direction thus facilitating a clockwise movement of water originating from

Fig. 1. Overview of North Dublin Bay and BI (Google Earth Pro).

the Atlantic Ocean — approximately 12 months for full replenishment (Fagherazzi, 2013). The estuary of the R. Liffey receives storm-water run-off from Dublin City, and treated wastewater from Ringsend wastewater treatment plant (WWTP). The Ringsend WWTP performs primary, secondary and partial tertiary treatments (UV screening) of sewage from Dublin City. Prior to the construction of underwater pipelines from south Dublin at Dunlaoighre in 1991 and north Dublin at Howth in 2001, wastewater from these areas were discharged to the bay after only basic screening.

In 1981, UNESCO declared BI as a biosphere reserve as it hosts internationally important habitats and species (Vestin, 2001). By 2015, the area included in the biosphere reserve had expanded throughout Dublin Bay and includes over 300 km (Dwyer, 2012) with a population of 300,000 people (UNESCO Biosphere Periodic Review Report, 2014). The sediments in BI and its surrounds are heterogeneous and can be divided into five zones; salt marsh (SM), mudflats (MF) that are submerged by the tidal waters in both the north and south lagoons, the golf courses (GC) on the main island (St Anne's and The royal Dublin), sand dunes (SD) and the intertidal zone (IZ) (Fig. 2). The two lagoon areas at the landside of BI, the SL and NL were a primary focus of this study, wherein, each lagoon consists of both vegetated SM and unvegetated MF zones. Each habitat is subjected to fundamentally differing hydrological regimes subsequently impacting sediment characteristics through long term processes. MF sediments are covered twice daily by incoming tides through all seasons and SM sediments receive tidal cover dictated by high tide levels, seasonal precipitation events influencing riverine loading and geographical positioning/ elevation. The saltmarsh (SM) zones contains a diversity of vegetation including *Salicornia sp*, *Halimione portulacoides, Puccinellia maritima, Zostera spp,* and *Spartina anglica* (Jeffrey et al., 1978b; Healy, 1975) and hosts Brent geese, while the tidal mudflats (MF) support wildfowl populations of national and international importance (Wilson and Forrest, 2005) (see Table 1). .

Table 1
Synopsis of intertidal primary production for communities in Dublin bay. Values are expressed in kg dry weight m^{-2} y^{-1} (Jeffrey and Hayes, 2005).

Biomass (above ground)	kg dW m^{-2} y^{-1}
Mudflat Fucoid algae	0.2–0.3
Green Algae	0.07–0.4
Microphytobenthos	0.03–0.1
Salicornia	0.5
Spartina	1
Zostera	0.1
Saltmarsh	3.0–4.0

2. Methodologies

2.1. Sampling strategy

A combination of ArcGIS (version 10.4) software and the GrTS (Generalised random Tessellation Stratified) package in r (version 3.4.1) provided sample locations with respective GPS co-ordinates (Stevens and Olsen, 1999). Within the defined BI catchment area, five distinct sampling zones were identified in ArcGIS (Fig. 2A), where a total of 63 locations were generated and 59 locations were subsequently sampled after the exclusion of 4 original locations due to logistical restraints (Excluded sample numbers 13, 58, 59 and 60 -Fig. 2B). Each zone had a selected number of samples assigned based on the likelihood of increasing variability between measured values for %OM (preliminary study of % OM content in zones, results not reported here). The five sampling zones and spatial sampling frequency were; mud flats (MF) = 24, salt marsh (SM) = 17, Golf Club (GC) = 7, sand dunes (SD) = 7 and intertidal zone (ITZ) = 8. Using the GrTS design package in r statistics, samples were then divided unequally into each sampling area. A higher number of samples was allocated to the mudflat and salt marsh areas where organic matter was expected to be higher. Sample descriptions are tabulated in Table SI.1.

Standard ArcGIS tools were used to generate and manipulate point, polyline and polygon data in all the map figures. Choropleth (graduated colour) mapping was applied in Fig. 2A, thus colour coding separate functional sub-regions of the study area for visualisation purposes. The same principle applied to classify quantities of chemical constituents in point symbol maps. Background satellite image maps and base maps were accessed from ArcGIS online mapping resource.

2.2. Sampling

Sampling was conducted in the summer months of 2016. MF, SM, SD and GC samples were taken by hand and sampling of the

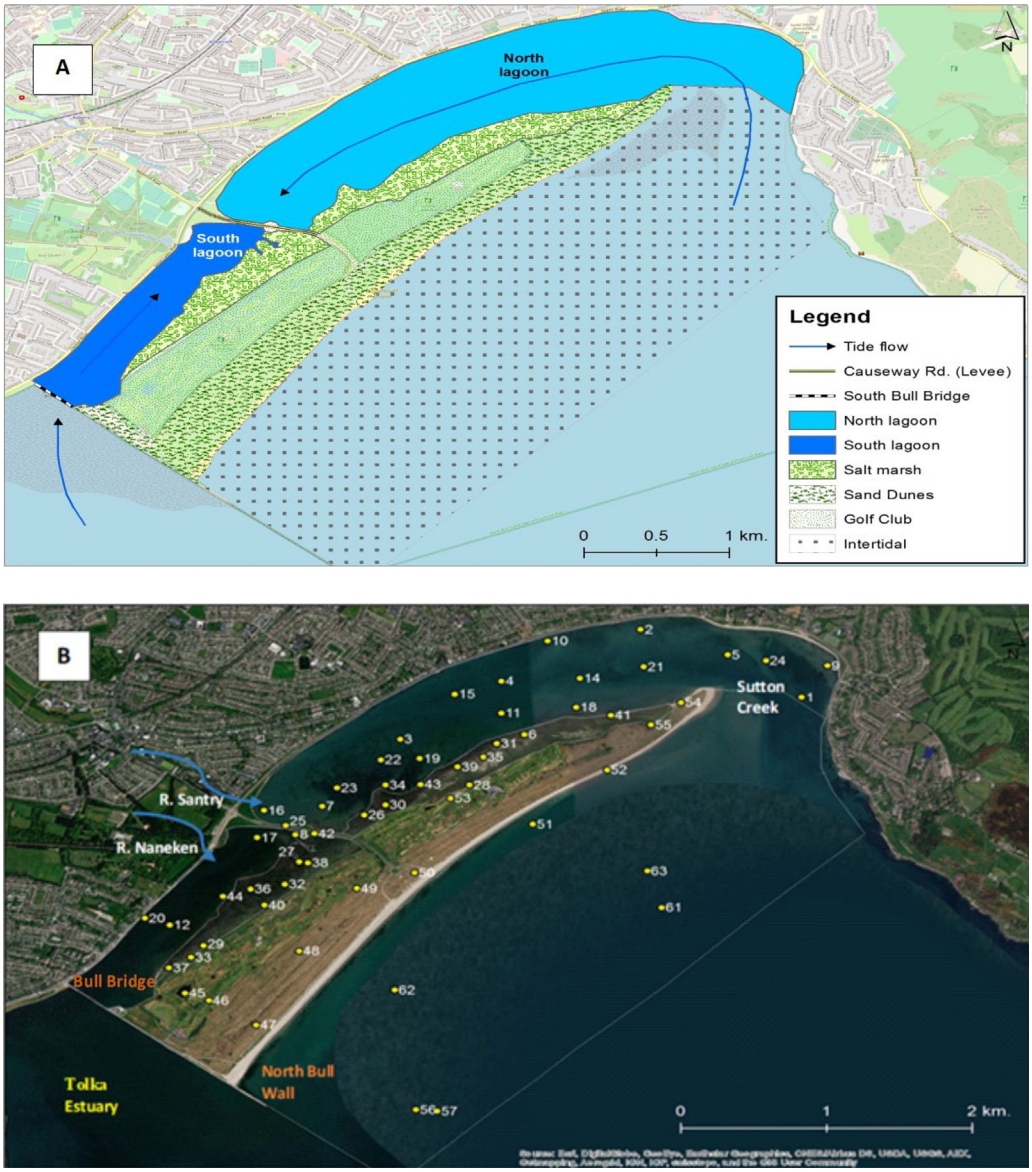

Fig. 2. A: Depiction of segregated zones of BI catchment area and surrounding hydrological processes and B: Overview of BI study area and the individual sampling points generated using Arc GIS.

ITZ was carried out on a small research vessel on an incoming tide using a Van Veen trap. Sample locations were identified using a handheld GPS. A 10 cm × 10 cm × 10 cm sample point was marked out using a trowel, which was rinsed with deionised water and acetone before each use. Two soil/sediment samples were extracted from each site to a 10 cm depth. The first sample was stored in a pre-labelled bag for physical, inorganic analysis and the second sample for organic analysis was stored in a pre-furnaced glass jar, with a PTFE lined lid. Samples were transported back to the lab and stored in a drawer freezer at −30 °C. Prior to sample preparation for all analysis, plant material, including roots were removed from vegetated sediments and algae biomass/debris was scraped from the surface of all MF samples. This step ensured that all sediments were analysed for materials integrated into the sedimentary matrix and thus allow comparison of accumulated sediment constituents representing longer term processes.

2.3. % SOil Organic Matter (SOM)

% SOM was determined by loss on ignition (LOI) (Vestin, 2001). Analyses were performed in triplicate on 3–5 g samples (previously dried from % moisture determination) for each site. Samples were sieved to >2 mm and ground using a mortar and pestle. Sediments were weighed into pre-weighed ceramic crucibles and ashed at 550 °C for 8 h. When cooled to room temperature, the mass of the crucible was subtracted from the total mass of the crucible/soil residue to obtain a mass of remaining inorganic compounds. The difference between inorganic and original mass, calculated as Δ Mass was determined to be the mass of OM lost during ignition, reported as a % of the original sample mass.

2.4. pH

Soil pH and EC were measured using the 5:1 method (soil:DiH_2O v/w) (Li et al., 2016), a Cyberscan PC300 series pH/meter (Eutech instruments) and a Thermo-scientific^{TM} Orion

star™ a222 conductivity portable meter. All samples were analysed in duplicate using 1–3 g of wet soil in tubes with appropriate water volume and placed on a horizontal shaker at 150 rpm for 60 min.

2.5. X-ray fluorescence (XrF) analysis of metals

A portable Thermo Scientific Niton XL3t XrF instrument was used for the determination of metal concentrations in soil samples. Instrument performance and protocols were validated in previous studies by Radu and Diamond (2009), also describing utilised methodologies (Radu et al., 2013; Radu and Diamond, 2009). Prior to analysis roots were removed by hand, sediments were oven dried (105 °C for 48 h), ground with a mortar and pestle, and sieved through a 0.85 mm sieve (International Atomic Energy Agency, 1997)

2.6. Particle size analysis (PSA) and elemental analysis

PSA was determined by laser granulometry using a Mastersizer 2000 particle size analyser (Malvern, Worcestershire, UK). Organic carbon (OC) was removed by furnacing at 550 °C for 6 h prior to analysis. PSA was determined for only 28 samples due to projects budgets and cost of outsourcing.

Elemental analysis was performed in triplicate using a Fisons NCS 1500 NA elemental combustion analyser. The instrument was calibrated using an Acetanilide (C_8H_9NO) standard before every batch of samples and after every 9 samples thereafter. Blank runs were performed after triplicate sets to eliminate possible carry over due to high %OM content. For CHN analysis, dried, ground and sieved sediment samples (0.85 mm) were weighed into tin capsules, sealed and combusted in the presence of O_2 to generated gaseous elements C, H and N, reported as % mass of initial sample. To determine %OC content, weighed samples were treated with 1M hydrochloric acid (HCL) in Ag capsules following the procedure of Verardo et al. (1990) to remove carbonate (Verardo et al., 1990), with subsequent measurements attained by combustion analysis.

2.7. Polyaromatic hydrocarbon (PAH) extraction

Samples were air-dried in the dark for 36–96 h (dependent on % organic matter), screened, homogenised and sieved to 420 μm particle size prior to extraction. The mass of sample chosen for extraction was dependent on the % OM content of individual samples. Sample weights between 3–5 g were suitable for higher OM samples (≥20% OM) and 5–7 g of sample was extracted for samples of lower OM content (≤20% OM). Final quantification was standardised to original sample mass used. All samples were extracted in triplicate.

Sediment samples were extracted using a Dionex Accelerated Solvent Extractor (ASE) (ASE® 200 Accelerated Solvent Extractor) instrument. A known mass of sample was briefly mixed with pre-furnaced sand and sodium sulphate before packing into 33 ml stainless steel extraction cells. Cells were assembled by capping one end (threaded steel cap with a Teflon lined opening for needle entry) and placing in a new cellulose filter disc. The sample was funnelled into the tube and a second filter was placed on top before sealing with an end cap and placing on the sample carousel. Dichloromethane (DCM) was injected into the extraction cell with subsequent heating to 100 °C and a hold time of 6 min. High purity nitrogen was then passed through the extraction cell at a pressure of 1500 psi, with subsequent collection of extractant solvent underneath in airtight and sterilised amber collection vials. Solvent entered the vials through a needle after piercing a new PTFE lined septum for every vial to reduce chances of cross contamination. The process included a 60% flush volume and a last purge of 60 s (Heemken et al., 1997). Each extraction cell was extracted for 1 full cycle and allowed to cool to room temperature. Sample extracts were reduced down (∼500 ul) at room temperature/low vacuum using rotary evaporation and made up to 1 ml in solvent washed round-bottom flasks. Finally, the 1 ml samples were transferred into pre-labelled GC vials and a spatula tip full of activated copper was added to the extracts to remove sulphur. The 1 ml extracts were shaken for 24 h in the dark and were then subsampled and stored upright at −30 °C until analysis.

2.8. Analysis of PAHs

Analysis of extracts was carried out on an Agilent 7890N gas chromatograph coupled to an Agilent 5973N mass selective detector operating in electron impact mode at 70 eV. The column was a 30 m HP-5MS column (0.25 mm i.d., 1 μm film thickness). The GC–Ms interface and ion source were set at 300 °C and 250 °C respectively. Selected ion mode (SIM) was used for analysis. The GC–MS method was set up as follows; the column flow rate was set to 1 ml/min, injection volume of 1 μl with a split ratio of 2:1 was set in conjunction with an injection port split liner. A solvent delay of 6 min was integrated into the method. The initial oven temperature was 70 °C for 0.5 min and increased at 10 °C/min to 300 °C and held for 20 min; with a total run time of 45 min. The data was processed using Chemstation software, combining mass spectral library databases (NIST and Wiley), certified PAH standards, spectra interpretation, retention times and referenced literature to confirm presence of identified compounds (Murphy et al., 2016). An internal standard of 100 ppm 5α-cholestane was used for all extracts and blanks. 16 priority PAHs were quantified in SIM mode using the cholestane internal standard and a calibration curve produced from a 16 PAH certified reference material standard. The limit of quantification (LOQ) and limit of detection (LOD) was calculated for each group of PAH compounds according to the number of benzene rings. A LOQ and LOD was determined for 2 ring PAHs using naphthalene, fluorene (3- ring), phenanthrene (4-ring), pyrene (5-ring) and benzo (ghi) perylene (6-ring). The LOQ for each PAH ranged from 22.50 ng/g (all 5 and 6-ring PAHs) to 67.50 ng/g (fluorene). The LOD ranged from 7.43 ng/g (all 5 and 6-ring PAHs) to 22.20 ng/g (fluorene).

A % recovery study was carried out using the described ASE method. Previously tested, PAH free sediment samples were spiked with the following deuterated PAH standards; naphthalene (d8), acenaphthene (d10), anthracene and perylene (d12) giving a recovery range of 75%–100%. recovery was determined using a range of sediment types (sand, mud and sandy mud) to represent the heterogeneity of samples from BI. The value for the sum of 16 priority PAHs at individual sample sites and subsequent zones was used to assign a PAH pollutant level classification as previously suggested by Baumard et al. (1998) as (a) low, 0–100 ng/g; (b) moderate, 100–1000 ng/g; (c) high, 1000–5000 ng/g; and (d) very high, >5000 ng/g.

Three PAH isomer pair ratios were applied to the data to elucidate possible PAH sources (Yunker et al., 2002);

1. indeno [1,2,3-c, d] pyrene/ (indeno [1,2,3-c, d] pyrene + benzo [g, h, i] perylene) (IP/IP+BghiP)
2. benzo[a]anthracene/(benzo[a]anthracene + chrysene) (BaA/228)
3. anthracene/(anthracene + phenanthrene) (An/178),

These ratios were plotted against the Fluoranthene/(Fluoranthene + Pyrene) (FL/Floppy) ratio to determine sources of PAHs in BI (Oros and Ross, 2004a). The PAH sources were determined as follows; IP/IP+BghiP ratio <0.20 — petroleum, 0.20–0.50

petroleum combustion, >0.50 — combustion of coal, grasses and wood. BaA/228 ratio <0.20 petroleum, 0.20–0.35 — petroleum and combustion, >0.35 — combustion, An/178 ratio <0.10 unburned petroleum sources, > 0.10 — combustion source. Fl/Fl+Py ratio <0.40 — petroleum, 0.40–0.50 — petroleum combustion, >0.50 — combustion of coal grasses and wood. Figure SI.10 shows the isomer ratio cross-plot for PAHs in BI; blue dots correspond to sample points. Areas where PAH concentration is below the LOQ could not be assessed for PAH source.

2.9. Data processing

Firstly, each of the measured geochemical properties was assigned a map where all 59 sample sites (from 5 defined zones across BI) were displayed as coloured points at respective GPS locations. The colour of any point at a location represented the mean measured values attained for a sediment property within a defined colour-value scale specific to the range of values attained for that geochemical property.

To achieve objectives and test the differences in geochemical characteristics between MF and SM sediments, and differences between NL and SL sediments, we defined four resolved study zones (2 pairs) identified in tidal affected regions within the lagoon areas of BI. The first pair of zones were mudflats (n = 24) and saltmarsh (n = 17), treated as composite sample groups independent of positioning in north and south lagoons i.e. all mudflat samples from north and south were grouped and all saltmarsh samples grouped the same. The second pair were the north (n = 27, larger area) and south lagoons (n = 14), areas physically segregated by a causeway structure, thus facilitating the introduction of different waters to respective lagoons. Individual sample site means for geochemical variables including PAH's were grouped according to positioning in defined zones, to generate descriptive statistics for the groups; 1. NL, 2. SL, 3. MF and 4. SM. Statistical analysis was carried out using IBM SPSS statistical package to test for significant differences between defined study groups across BI — north vs south lagoons and mudflats vs saltmarsh zones. Data sets were tested for normality and the Mann Whitney U test, a non-parametric test was chosen as it does not assume data to be normally distributed. The Mann Whitney U test utilises a Mean rank (the test output when data has violated 'assumption 4' of the Mann Whitney U test) e.g. A higher mean rank for a variable on the south zone of the island versus the north zone for the same variable indicates a higher value for this variable e.g. A higher mean rank for % organic matter (OM) on the south vs north. However, the mean rank is not the true mean value of the data set measured for the variable, but instead a proxy value representing the value of the mean with respect to all data within a set. The significance of the differences is indicated by the p value where, a critical value p = 0.05 (95% confidence level) is utilised in the statistical output file. Spearman's correlation analysis was applied to the combined south and north lagoon data set (saltmarsh and mudflat data) to explore relationships between measured variables in the tidal impacted zones and verify the influence of OM components on the distribution of PAHs and metals. It must be acknowledged that the current study represents a snapshot of geochemical sediment characteristics at the time of sampling. However, due to a sampling depth of 10 cm the results can be considered to represent longer term or decadal hydrological processes, sedimentation, marsh accretion, vegetation growth and microbiological carbon cycling.

3. Results and discussion

3.1. Bulk physical and chemical analysis overview

Mean results for all measured geochemical sediment properties at individual sites were tabulated and used to generate point symbol maps to visualise distributions of values. (Tables SI.4, SI.5 and Fig. SI.1 –SI.8). GC, SD and INTZ mean results (Table SI.5) are not discussed in detail throughout as the main focus of the study is on the tidal wetland zones of the lagoons and the influence of long term riverine inputs on sediment geochemistry. However, brief references are made to the GC, SD and INTZ zones to put in context the geographical positioning of the tidal lagoons and differences in hydrological dynamics.

3.2. MF and SM sediment geochemistry

Higher concentrations of most of the bulk chemistries tested in the SM relative to MF sediments is a reflection of the efficiency of sediment deposition on elevated SMs. Deposition is enhanced by the physical trapping of silts, clays and OM particulate inputs by vegetation leaves, shoots and roots (Fig. 3A and 3B). Carbon accumulates in the soil over time where burial and anoxic conditions transforms it into increasingly recalcitrant organic matter (Ouyang and Lee, 2014). Studies also show the efficiency of vegetated wetlands to accumulate metals in the rhizosphere soil (Doyle and Otte, 1997) and the involvement of these metals in stabilising OM through formation of organometallic ligands, thus potentially enhancing the longer term storage of carbon (Jokic et al., 2003; Bhattacharyya et al., 2019; Stumpner et al., 2018). TOC ranged from 001–15.95% and is significantly higher in vegetated SM sediments (6.24%) than the sandier MF zones (1.06%) and this is reflected by the same trend in %OM (SM = 22.51 and MF = 4.32). The %OM values agree with similar results reported by Doyle and Otte (1997) for BI, where SM sediments had values ranging from 19.1 to 24.3% and 1.6 to 3.5% for MF sediments, attained after LOI.

TN correlated strongly positively to OM and TOC, however the relationship with clays and silts was strongest (p<0.001) where concentrations were significantly highest in the SM zone, suggesting a N exchange dynamic with inorganic particles. Over 95% of N in sediments can exist as organic N arising from immobilisation through plant, algae and microbial biomass, predominantly in the form of proteinaceous debris (Bingham and Cotrufo, 2016). Microbial mineralised N in sediments is generally released as ammonia (NH_4^+) where it can undergo numerous processes — some of which include direct uptake by algae, microbes or plants, loss to the atmosphere, and attachment to negatively charged surfaces such as silt or clay. Furthermore, plants in SM sediments promote the oxidation of NH_4^+ by root oxygen diffusion for NO_2^- uptake, which invariably increases sediment acidity (Nieder et al., 2011), demonstrating links between cycling of nutrients and metals facilitated by rhizosphere horizons. The total organic carbon to nitrogen ratio (C/N ratio) in soils and sediments is a useful proxy that is employed in paleo-climatic (Ishiwatari and Uzaki, 1987), agricultural (Friedel and Gabel, 2001), composting (Barrington et al., 2002), marine and sedimentary research (Rumolo et al., 2011; Kähler and Koeve, 2001). In coastal environments where organic matter will come from several sources, the C:N ratio helps us establish whether OM is terrestrial (C:N ratios generally higher than 15) or marine (C:N between 4 and 15) in origin (Meyers, 1997). The ratio of TOC to total nitrogen content (C:N) varied across the tidal wetland area, between 2.0 and 175 (Fig. SI.1B). Highest C:N values (terrestrial material) are seen in areas of higher silt, particularly in the saltmarsh and mudflats (near the road) to the north and saltmarsh just south of the causeway.

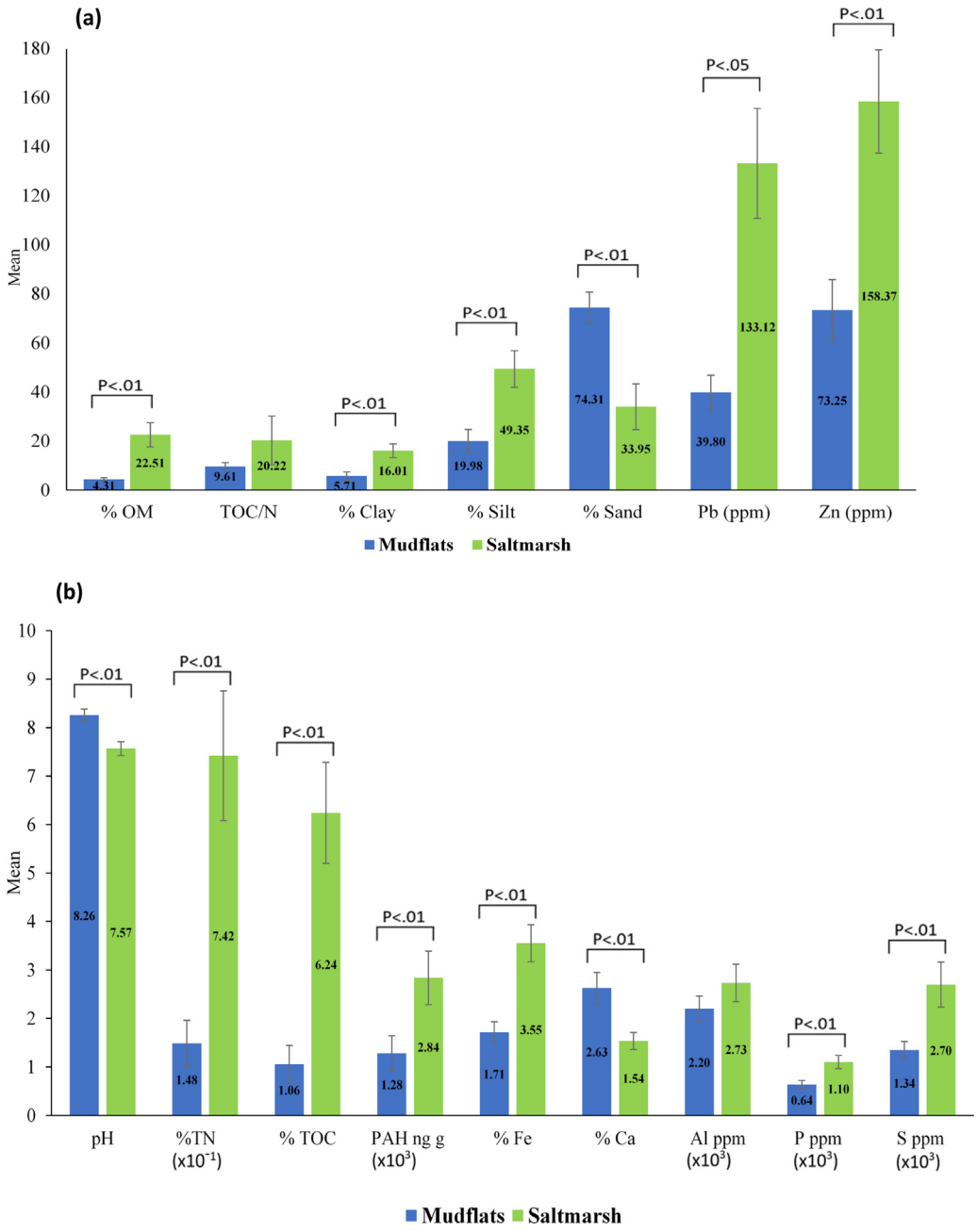

Fig. 3. (a) and (b): Bar charts representing mean values of all sediment geochemistry's measured in MF and SM zones. Error bars represent standard error. Significant differences and alpha level for a geochemical measurement between zones are indicated over the respective groups. Scientific notation was used with variables in graph (b) to scale data while maintaining original units.

Overall, MF sediments had a mean C:N of 9.60 indicating marine or algal values, contrasting to the vegetated SM mean of 19.66, albeit the MF sediments had far lower variability than the SM (± 1.57 and ± 10.01 respectively). Previous studies have identified the C:N of saltmarsh vegetation shoot and root biomass (e.g. *Salicornia virginica* 16.2 ± 0.7 {succulent} and *Spartina Alterniflora* 31.1 ± 2.0 {grass}) with much variation across plant species, more profound in detritus through different stages of degradation (Radabaugh et al., 2016; Lanari et al., 2018).

Ca was significantly higher ($p<0.01$) on the MF zone, likely associated with marine biogenic calcification and subsequent long term accumulation of debris. High Fe concentrations are mostly associated with the high OM saltmarsh soils ($p<0.01$) (Fig. SI.3 A), as was previously found by Doyle and Otte (1997), who determined that Fe and As concentrations were significantly higher in vegetated/inhabited soils, where Fe plaque was evident at the root sediment interface (Doyle and Otte, 1997). Higher iron in the SM may reflect the strong association of Fe and C in coastal and marine sediments (Barber et al., 2017). The preservation of organic matter in sediments is strongly associated with binding to reactive iron phases, a link that is known as the "rusty sink" (Eglinton, 2012) These processes are further enhanced in pH fluctuating sediments associated with the rhizosphere region of saltmarsh vegetation (Sokol et al., 2019). This metal and biomass relationship is supported by significantly positive correlations between %OM (all with $r>0.6000$, $P<0.01$) and total metals; Fe, P, Pb, Zn and S (Long et al., 1998; Frid, 2003). Conversely, positive relationships between Fe, Pb, and Zn displayed higher and more significant inter-relationships than with C. This suggests a high

binding capacity of Fe for other metals, a process known to be enhanced under conditions suitable for Fe-oxide production (Zhang et al., 2014). Indeed, SM (pH = 7.57) sediments had significantly lower mean pH (P<0.01) than MF sediments (pH = 8.26).

Previous studies of saltmarsh sediments have discussed seasonal fluctuations of metal speciation in root zones, more specifically in the rhizospheres of *Salicornia*, *Halimione, Puccinellia* and *Spartina* (Sundby et al., 2003) (Hung and Chmura, 2007; Duarte et al., 2010), demonstrating that Pb cycling is controlled by seasonal growth and decay of vegetation roots. In summer, root delivered O_2 causes oxidation of Fe(II) and lead bearing phases, thus facilitating Fe-oxide formation and release of Pb(II) for plant uptake. During winter–spring, roots decay and Pb is precipitated into the anoxic sediments where binding with OM and sulfides occurs. The presence of vegetation in BI sediments, more specifically belowground biomass, indicates high potential for metal retention, facilitated by root, microorganism and sediment exchanges imparting redox controls on metal speciation at localised scales. The results of bulk metal analysis in this study thus reflect evidence of longer term fate of metals at a broader spatial scale after entering wetland sediments. The strong relationships between OM and metals demonstrates the role of biomass, thus organic matter inputs in exerting both direct (binding capacity) and indirect (changes in redox and pH during biogeochemical cycling) influences on metal retention.

3.3. PAH sources and distributions in MF and SM sediments

PAH isomer pair ratio plots suggest that most PAHs come from the combustion of biomass and fossil fuels, with a small amount coming directly from petroleum and oil (Fig. SI.11). The first isomer ratio calculation (IP/IP+BghiP) shows that many PAHs are present from biomass and coal combustion. The second isomer ratio calculation (BaA/228) also showed that the PAHs in a large number of samples came from combustion except sample 46 taken from the island, which suggests a direct petroleum source. The same trend occurred for the final isomer ratio (An/178), with one more sample, number 49, again coming from the island, showing petroleum as a source. These results are in agreement with reported sources in a previous study of Dublin bay by Murphy et al. (2016) where sediments were sampled on a transect of the R. Liffey channel plume. The highest total PAH value in this study for a single sample was 3072 ng/g, while the mean recorded value for 30 samples was 540 ng/g. The authors attributed the distributions to historical deposition from the R. Liffey and untreated sewerage from Howth.

Total PAH was significantly (P<0.01) higher in the SM (2748.97 ng/g) than the MF (1282.77 ng/g), with both zones under the high PAH classification index (high, 1000–5000 ng/g. The mean for total PAH sdw on all tidal impacted lagoon zones was 2117.10 ng/g, also classified as high PAH contamination. The highest recorded PAH value of 8183.0 ng/g is classified as very high and was recorded in the MF sediments just north of the causeway likely associated with the entry point of the R.Santry. The following were the numbers of MF sample sites (n = 24) classified under each pollution level: 2 = low, 14 = moderate, 7 = high and 1 = very high. The SM sediments (n = 17) had a higher incidence of elevated PAH concentration at individual sites with the following: 1 = low, 3 = moderate, 9 = high and 4 = very high. Similarly, to the distribution of metals in BI's sediments and reported in many studies (Gonçalves et al., 2016; Martins et al., 2008), elevated PAH accumulation occurred at vegetated sites with higher TOC, reflected in a strong and significant relationship (r = 0.6080, P<0.01). Interestingly, total PAH had a weak but significant relationship to silt (r = 0.4015, p<0.05), but a statistically stronger (p<0.05) association existed with $\sum$ 4 ring (r = 0.4031) and 5 ring (r = 0.4439) PAH's and silt. Similar strong relationships between PAH and silt have been previously reported in Dublin Bay (Murphy et al., 2016).

Effects range low (ErL) and effects range median (ErM) concentrations have been used as numerical predictor values for toxicity in marine sediments. ErL and ErM values for low molecular weight (LMW) PAHs (2–3 ring) are 550 ng/g and 3160 ng/g respectively, while high molecular weight (HMW) PAHs (4–6 ring) are 1700 ng/g and 9600 ng/g respectively. ErL and ErM values for total PAH (16 priority PAHs) are 4022 ng/g and 44790 ng/g respectively (Long et al., 1998; Frid, 2003). Mean values for SM and MF sediments were below the ErL, however, there were 5 sites on the SM and 1 site on the MF with total PAH levels falling in the ErL to ErM range (Table SI.1).

A higher TOC content in saltmarsh sediments can facilitate the accumulation of higher concentrations of PAHs due to a high affinity for sorption to organic matter (Vane et al., 2007). While most PAHs have a low aqueous solubility and therefore low mobility, they are attracted to fine organic-rich particulates (Walker et al., 2013). The solubility and biodegradation of PAHs decreases generally as molecular mass increases and smaller 2–3 ringed PAHs can dissolve in water, making them more susceptible to biological uptake and degradation (Mackay and Callcott, 1998). Significantly higher TOC content in the SM zone is the likely reason why we see significantly higher means for the 4, 5, and 6 ring PAH's and a higher % contribution of 5–6 rings to total PAH when compared to the MF where % 2–3 ring and % 4 ring contributions are highest (Fig. 4). HMW PAHs are lipophilic in nature, thus sequestration is enhanced in water logged, high OM and low pH sediments of the SM (Fig. 5).

The MF zone is fundamentally different with low elevation, daily surface flooding, high light exposure and lack of vegetation. Sediment %OM is significantly lower on the MF, thus we see less accumulation of strongly correlating metals and PAHs. Conversely, during summer periods nutrient availability and increased light creates conditions suitable for excessive algae growth across MF zones (SI.12 (a)- winter and (b) - summer). While the bulk sediments in MF zones may show lower C accumulation, these highly exposed and porous sediments successfully support high aboveground algal biomass actively utilising water column nutrients to initiate C capture. Algae blooms on BI's MF's are a seasonal event, however, the growth and death of biomass plays a large role in immobilisation of C, N, P, and S through natural cycles while subsequent necromass may be distributed across the SM, subsequently integrating into sediments. Macroalgal contributions to blue carbon stocks have been increasingly acknowledged in recent times (Krause-Jensen and Duarte, 2016).

4. North and south lagoon zones

4.1. Impacts of estuarine system on north and south lagoons

BI's NL and SL zones initially existed as one lagoon with a SM zone of 200 meters in breadth spanning the length of BI's landside coastline. Tidal waters entering from channels at either end of the island previously mixed in the lagoons, facilitating dispersal and deposition of water borne particles along the length of the lagoon shoreline. The construction of a causeway in 1964 at meeting points of waters saw the emergence of two lagoons. The SL is directly connected to the Tolka/Liffey estuaries through a channel passing under Bull bridge and this smaller lagoon receives tidal waters from the Liffey and Tolka rivers and to a lesser extent from the Naneken river. The NL is connected to Dublin Bay via Sutton Creek and the Santry river culverts along stretches of varying lengths with unspecified run-offs from roads

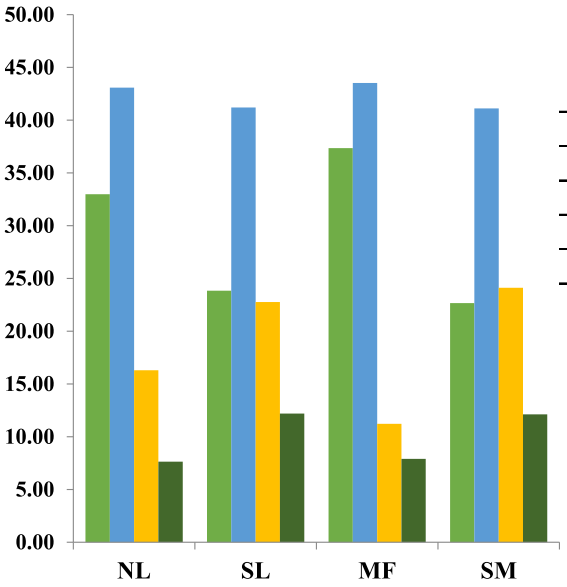

% Contribution to total PAH (ng/g)

Zone	2-3 ring	4 ring	5 ring	6 ring
NL	32.97	43.09	16.30	7.64
SL	23.84	41.20	22.76	12.20
MF	37.35	43.53	11.22	7.90
SM	22.66	41.11	24.11	12.12

Fig. 4. % contribution of grouped ring structure PAHs to total PAH in tidal influenced NL, SM, MF and SM zones of BI.

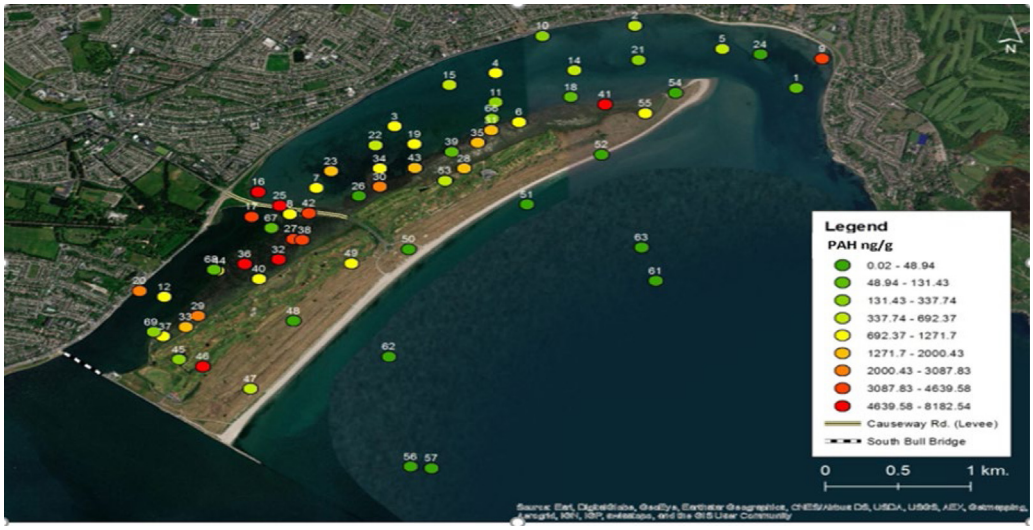

Fig. 5. Distribution of total PAH ng/g across BI.

and former industrial areas (Fig. 1) but has a small impact on the water flow in this area. The NL receives seawaters with a much higher silt content from the R.Liffey plume and the Irish Sea where the large size of the lagoon allows the waters to slow down completely, facilitating significant sediment deposition of lower density particles (David Jeffrey and Nairn, 2017). In each lagoon zone, SM expansion and MF regions have been physically shaped to reflect hydrological processes imparted since the construction of the causeway. Fundamentally, when organic and inorganic materials enter either lagoon zone, the biogeochemical cycling occurring at the water–sediment interface is constrained by similar processes. However, where long term deposition of materials is dictated by geographical positioning, fluvial transportation, fluctuating loading rates and different chemical inputs, the accumulative effects of differences in water sources will be reflected in sediment geochemistry.

We aimed to determine if there were differences in the measured sediment geochemistry between the SL connected to an estuarine system and the NL receiving waters with higher marine mixing. This was hypothesised to occur as a consequence of riverine impact on wetland receiving tidal waters. The SL had significantly ($P<0.05$) higher measurements for TOC, OM, TN and PAHs than the NL together with higher mean concentrations of Pb, S, P, Zn, clay and silt, while pH was significantly ($P<0.01$) lower in the SL (Figs. 6a and 6b). Ca, Fe and Al had higher mean concentrations in the NL sediments. These results suggest that a direct connection to the estuarine zone exerts a significant influence on the SL sediments, predominantly through elevation of OM constituents and contaminant levels.

Previous studies of Dublin coastal zones have extensively reported on the dynamics of particulate matter and dissolved-nutrients inputs to the Bay, highlighting their contribution to algal growth though remineralisation (O'Higgins and Wilson, 2005; Wilson et al., 2002; Jeffrey et al., 1995).Sewage discharge, rivers and canals have been reported to contribute largely to suspended particulate matter (SPM) in the estuarine system, aided by the hydrodynamics of the Bay which limit external particulate transport. Data records from the bay indicate that one tidal prism has been shown to carry dissolved nutrient levels equal to an entire day of river contributions (Dabrowski et al., 2012; McGovern et al., 2002). Thus, incoming tidal flush drives SPM, fluvial

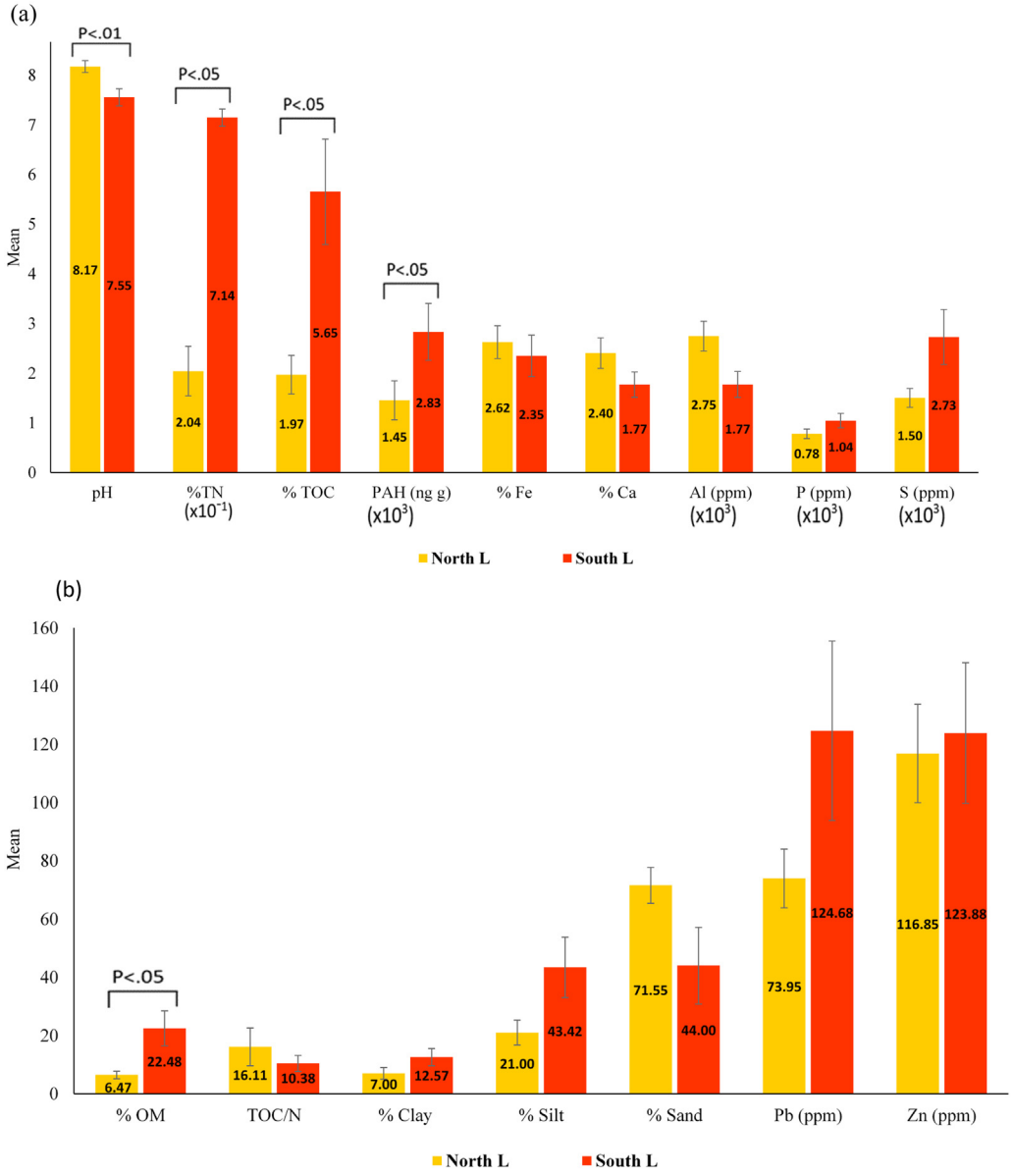

Fig. 6. (a) and (b): Bar charts representing mean values of all sediment geochemistrys measured in MF and SM zones. Error bars represent standard error. Significant differences and alpha level for a geochemical measurement between zones are indicated over the respective groups. Scientific notation was used with variables in graphs to scale data while maintaining original units.

sediments and dissolved nutrients into the upper Liffey and Tolka estuaries. Sediment is deposited and retained due to the internal circulation between the retaining sea walls in Dublin Port (Buggy and Tobin, 2006). Supporting this process, when compared with the NL, the results for fluvial contributions of % silt and % clay on BI's lagoons show over twice the content in the SL sediments, coinciding with three times the levels of OM and TN. Contrary to this, in the NL zone adjacent to the causeway, a large area of emerging *Salicornia* sp. marsh is facilitating increased deposition of silt particles (David Jeffrey and Nairn, 2017). This phenomenon is enhanced by lower water energy in the relatively larger area of the NL at 310 ha compared to the SL where the area is an estimated 78 ha.

The lagoon zones produce seasonal macroalgal blooms, generally beginning in April and peaking in August, with previous reports of over double the biomass on the MFs of the SL (see Fig. SI.12 for visual comparison of lagoons). The sedimentation of SPM, has been strongly implicated as the major supply of N for algal blooms in BIs lagoons, subsequently a focus of two remineralisation hypotheses by Jeffrey et al. (1995). They provided evidence of a nutrient difference between the NL and SL through research that shows that in the NL, nitrogen levels in algal biomass can fall below the growth threshold of 2%, due to lowest water dissolved N levels in the summer (Kunikane et al., 1984). Our results support this observation as the SL sediments had a mean C/N value of 10.38, which was strikingly close to the previously discussed MF value of 9.62. This is compared to the NL value of 16.11, which was more comparable to the C/N of the SM zone (20.22). This indicates SL sediments had more labile OM, higher N stocks and potential for ammonification, which has been identified as the dominant source of soluble N supply in water–sediment exchange. This is most likely a result of imported SPM; however, it is expected that contributions come from an internal supply of N due to SM sediment leaching and remineralisation of algal necromass. The distribution of necromass may also explain relatively higher bulk S and P concentrations in the SL sediments, as a result of historical accumulation.

PAH and metals (Pb and Zn) reach higher levels in the SL sediments, likely enhanced by estuary supply. Similarly, this reflects previous work (Buggy and Tobin, 2006; Choiseul and Nixon, 1998; Brennan, 1991) that reported highest concentrations of organic contaminants and metals in sediments of the inner parts of the harbour and Tolka estuary. Both NL and SL zones were classified under high level PAH pollution at 1452.46 ng/g and 2831.25 ng/g respectively. Indeed, concentrations of lead (Fig. SI.4B) are over five times WHO permissible limits (Hassaan et al., 2016) for Pb in soil (85 mg/kg) at 439 mg/kg in one southern saltmarsh sample and reach concentrations that are at least 1.5 to two times recommended levels at 19 sites, especially both sides of the causeway (Table SI.4). Zinc also exceeds the WHO recommendation of 50 mg/kg in soil on 31 occasions with values exceeding 250 mg/kg again mostly both sides of the causeway in both lagoons and on the island (Fig. SI.5B).

5. Conclusion

The results of this study demonstrate the influence of both higher riverine and anthropogenic inputs to blue carbon sediments over 50 years of tidal deposition and marsh accretion. While by no means exhaustive, the results contribute to our understanding of the source and fate of marine and terrestrial inputs and how such a dynamic ecosystem sustains itself and grows. The study investigated geochemical properties of two contrasting sediments within a blue carbon system — SM and MF sediments. SM sediments accumulated significantly higher mean levels of OM, TOC, N, P, PAH's, silts, clay and metals, including Fe, S, Zn and Pb. MF sediments contained significantly higher Ca, elevated Al and a significantly higher mean pH. However, lower OM in the MF does not reflect the high autotrophic productivity of the sediment surfaces where dense algae growth is seasonally enhanced presumably through capture of elevated river exports of nutrients, with compelling evidence in the SL zone. MF primary productivity may be a significant contributor to long term stocks of OM, more specifically N within the SM zones through necromass distribution, while also initiating metal and pollutant capture within the water column. SL and NL zones were also compared using the same data set. The results suggest that a direct connection to the estuarine zone exerts a significant influence on the SL sediments. In the SL, significantly higher means were recorded for OM, TOC, N, total PAH, and also for 4,5, and 6 ring PAHs, all coinciding with a significantly lower mean pH. Silt and clay distributions were also higher in the SL, albeit SM expansion in the NL is facilitating increased capture. The establishment of BI as a blue carbon capture zone is a direct result of anthropogenic diversion of natural processes aided by hydrologically constrained distribution of process outputs (Mathew et al., 2019) and succession of resilient biota.

Future studies must put extensive focus on studying the dynamics of 'outwelling' and internal cycling of sediment chemistry to evaluate: (1) autotrophic contributions to OM accumulation including the impact of different species of vegetation and algae, (2) investigate and interpret sediment microbiology, (3) determine and monitor the scale of synthetic anthropogenic input, (4) determine accurate estimates of historical, current and potential C sequestration within these sediments, and (5) evaluate the potential contribution of SM sediment outwelling or leaching to biological productivity during climatic events e.g. drought periods and rainfall. The heterogeneity of the area provides excellent opportunities to validate and verify remote sensing technology that can be used to understand and predict coastal change. Future work should evaluate the carbon sequestration capacity of BI as a model representative and its potential to grow vertically to avoid sea level rise could be assessed. From a geological perspective, these are young sediments that have captured decades of modern anthropogenic waste whilst maintaining growth and productivity. BI and other similar zones globally represent blue carbon sediments with increasing retention of natural and anthropogenically derived materials including plastics, phthalates, pharmaceuticals and PAHs. Thus, future blue carbon stocks in such regions may possess vastly different chemical signatures from older blue carbon sediments. Questions may arise as to the long term impact of such inputs on vegetation, microbial processes, leaching and ultimately, the balance between C mineralisation and sequestration. This knowledge will not only be very important for our management of such important ecosystems but also for the potential of engineered sediment capture that stores carbon and protects coasts.

Declaration of competing interest

The authors declare that they have no known competing financial interests or personal relationships that could have appeared to influence the work reported in this paper.

Acknowledgements

The authors would like to thank Science Foundation Ireland (Investigator Programme, grant number 16/IA/45209) and the Irish Research Council (grant numbers EPSPD/2015/20 and EPSPG/2015/63) for funding this project.

Appendix A. Supplementary data

Supplementary material related to this article can be found online at https://doi.org/10.1016/j.rsma.2021.101834.

References

Alongi, D.M., 2002. Present state and future of the world's mangrove forests. Environ. Conserv. 29, 331–349.
Barber, A., et al., 2017. Preservation of organic matter in marine sediments by inner-sphere interactions with reactive iron. Sci. Rep. 7.
Barrington, S., Choinière, D., Trigui, M., Knight, W., 2002. Effect of carbon source on compost nitrogen and carbon losses. Bioresour. Technol. 83, 189–194.
Baumard, P., Budzinski, H., Garrigues, P., 1998. Polycyclic aromatic hydrocarbons in sediments and mussels of the western Mediterranean sea. Environ. Toxicol. Chem. 17, 765–776.
Bhattacharyya, A., Schmidt, M.P., Stavitski, E., Azimzadeh, B., Martínez, C.E., 2019. Ligands representing important functional groups of natural organic matter facilitate Fe redox transformations and resulting binding environments. GeCoA 251, 157–175.
Bingham, A.H., Cotrufo, M.F., 2016. Organic nitrogen storage in mineral soil: Implications for policy and management. Sci. Total Environ. 551–552, 116–126.
Brennan, B., 1991. Chemical partitioning and remobilization of heavy metals from sewage sludge dumped in Dublin Bay. Water Res. 25, 1193–1198.
Brooks, P.R., Nairn, R., Harris, M., Jeffrey, D., Crowe, T.P., 2016. Dublin Port and Dublin Bay: Reconnecting with nature and people. Reg. Stud. Mar. Sci. Part 2, 234–251.
Buggy, C.J., Tobin, J.M., 2006. Seasonal and spatial distributions of tributyltin in surface sediment of the Tolka Estuary, Dublin, Ireland. Environ. Pollut. 143, 294–303.
Cachot, J., et al., 2006. Evidence of genotoxicity related to high PAH content of sediments in the upper part of the Seine estuary (Normandy, France). Aquat. Toxicol. 79, 257–267.
Castillo, J.M., Luque, C.J., Castellanos, E.M., Figueroa, M.E., 2000. Causes and consequences of salt-marsh erosion in an Atlantic estuary in SW Spain. J. Coast. Conserv. 6, 89–96.
AR5 climate change 2014: Impacts, adaptation, and vulnerability–IPCC. https://www.ipcc.ch/report/ar5/wg2/.
Choiseul, V., Nixon, E., 1998. The distribution of hydrocarbons on the east and south-west Irish in the Liffey. Estuar. Coasts 98, 75–86.
Costanza, R., et al., 2008. The value of coastal wetlands for hurricane protection. Ambio 37, 241–248.
Cott, G.M., Caplan, J.S., Mozdzer, T.J., 2018. Nitrogen uptake kinetics and saltmarsh plant responses to global change. Sci. Rep. 8, 5393.

Dabrowski, T., Hartnett, M., Olbert, A.I., 2012. Determination of flushing characteristics of the Irish Sea: A spatial approach. Comput. Geosci. 45, 250–260.
David Jeffrey, R.G., Nairn, Richard, 2017. Dublin Bay, Nature and History. The Collins Press.
Doyle, M.O., Otte, M.L., 1997. Organism-induced accumulation of iron, zinc and arsenic in wetland soils. Environ. Pollut. 96, 1–11.
Duarte, B., Caetano, M., Almeida, P.R., Vale, C., Caçador, I., 2010. Accumulation and biological cycling of heavy metal in four salt marsh species, from Tagus estuary (Portugal). Environ. Pollut. Barking Essex 1987 158, 1661–1668.
Dwyer, N., 2012. The Status of Ireland'S Climate, Vol. 2012. pp. 1–157.
Eglinton, T.I., 2012. Geochemistry: A rusty carbon sink. Nature 483, 165–166.
Fagherazzi, S., 2013. The ephemeral life of a salt marsh Sergio. Geology 29, 587–590.
Fourqurean, J.W., et al., 2012. Seagrass ecosystems as a significant carbon stock. Nat. Geosci. http://dx.doi.org/10.1038/ngeo1477.
Frid, C., 2003. Bioaccumulation in marine organisms. Effect of contaminants from oil well produced water. Org. Geochem. 34, 149.
Friedel, J.K., Gabel, D., 2001. Microbial biomass and microbial C:N ratio in bulk soil and buried bags for evaluating in situ net N mineralization in agricultural soils. J. Plant Nutr. Soil Sci. 164, 673–679.
Gedan, K.B., Kirwan, M.L., Wolanski, E., Barbier, E.B., Silliman, B.R., 2011. The present and future role of coastal wetland vegetation in protecting shorelines: answering recent challenges to the paradigm. Clim. Change 106, 7–29.
Gonçalves, C., Teixeira, C., Basto, M.C.P., Almeida, C.M.R., 2016. PAHs levels in portuguese estuaries and lagoons: Salt marsh plants as potential agents for the containment of PAHs contamination in sediments. Reg. Stud. Mar. Sci. 7, 211–221.
Hassaan, M.A., Nemr, A.E., Madkour, F.F., 2016. Environmental assessment of heavy metal pollution and human health risk. Am. J. Water Sci. Eng. 2, 14–19.
Healy, B., 1975. Fauna of the Salt-Marsh, North Bull Island, Dublin. Proc. R. Ir. Acad. B 75, 225–244.
Heemken, O.P., Theobald, N., Wenclawiak, B.W., 1997. Comparison of ASE and SFE with soxhlet, sonication, and methanolic saponification extractions for the determination of organic micropollutants in marine particulate matter. Anal. Chem. 69, 2171–2180.
Hung, G.A., Chmura, G.L., 2007. Metal accumulation in surface salt marsh sediments of the Bay of Fundy, Canada. Estuar. Coasts 30, 725–734.
International Atomic Energy Agency, 1997. Sampling, storage and sample preparation procedures for X ray fluorescence analysis of environmental materials.
Ishiwatari, R., Uzaki, M., 1987. Diagenetic changes of lignin compounds in a more than 0.6 million-year-old lacustrine sediment (Lake Biwa, Japan). Geochim. Cosmochim. Acta 51, 321–328.
Jeffrey, D.W., Brennan, M.T., Jennings, E., Madden, B., Wilson, J.G., 1995. Nutrient sources for in-shore nuisance macroalgae: The Dublin Bay case. Ophelia 42, 147–161.
Jeffrey, D.W, Hayes, M., 2005. Net primary productivity of intertidal systems: the Dublin bay example. In: Wilson, James (Ed.), THE INTERTIDAL ECOSYSTEM:THE VALUE OF IRELAND'S SHORES, 1st ed. 1. Royal Irish Academy, Dublin, pp. 45–47.
Jeffrey, D.W., Pitkin, P.H., West, A.B., 1978a. Intertidal environment of Northern Dublin Bay. Estuar. Coast. Mar. Sci. 7, 163–171.
Jeffrey, D.W., Pitkin, P.H., West, A.B., 1978b. Intertidal environment of Northern Dublin Bay. Estuar. Coast. Mar. Sci. 7, 163–171.
Jokic, A.V., Cutler, J.N., Ponomarenko, E., Kamp, G., van der, Anderson, D.W., 2003. Organic carbon and sulphur compounds in wetland soils: insights on structure and transformation processes using K-edge XANES and NMR spectroscopy. http://dx.doi.org/10.1016/s0016-7037(03)00101-7.
Kähler, P., Koeve, W., 2001. Marine dissolved organic matter: can its C:N ratio explain carbon overconsumption? Deep Sea Res. Oceanogr. Res. Pap. 48, 49–62.
Kelleway, J.J., et al., 2017. Geochemical analyses reveal the importance of environmental history for blue carbon sequestration. J. Geophys. Res. Biogeosci. 122, 1789–1805.
Kennedy, H., et al., 2010. Seagrass sediments as a global carbon sink: Isotopic constraints. Glob. Biogeochem. Cycles 24.
Kim, K.H., Jahan, S.A., Kabir, E., Brown, R.J.C., 2013. A review of airborne polycyclic aromatic hydrocarbons (PAHs) and their human health effects. Environ. Int. 60, 71–80.
Krause-Jensen, D., Duarte, C.M., 2016. Substantial role of macroalgae in marine carbon sequestration. Nat. Geosci. 9, 737–742.
Kristensen, E., Bouillon, S., Dittmar, T., Marchand, C., 2008. Organic carbon dynamics in mangrove ecosystems: A review. Aquat. Bot. 89, 201–219.
Kunikane, S., Kaneko, M., Maehara, R., 1984. Growth and nutrient uptake of green alga, scenedesmus dimorphus, under a wide range of nitrogen/phosphorus ratio—I. Experimental study. Water Res. 18, 1299–1311.
Lanari, M., Claudino, M., Garcia, A., Copertino, M., 2018. Changes in the elemental (C, N) and isotopic (δ 13 C, δ 15 N) composition of estuarine plants during diagenesis and implications for ecological studies. J. Exp. Mar. Biol. Ecol. 500, 46–54.
Li, X., Wang, X., Zhao, Q., Zhang, Y., Zhou, Q., 2016. In situ representation of soil/sediment conductivity using electrochemical impedance spectroscopy. Sens. Switz. 16, 1–9.
Liu, N., et al., 2017. Distribution, sources, and ecological risk assessment of polycyclic aromatic hydrocarbons in surface sediments from the Nantong Coast, China. Mar. Pollut. Bull. 114, 571–576.
Long, E.R., Bin, C., Macdonald, D.D., Smith, S.L., Calder, F.D., 1995. Chemical concentrations in marine and estuarine sediments. Environ. Manage. 19, 81–97.
Long, E.R., Field, L.J., MacDonald, D.D., 1998. Predicting toxicity in marine sediments with numerical sediment quality guidelines. Environ. Toxicol. Chem. 17, 714–727.
Loomis, M.J., Craft, C.B., 2010. Carbon sequestration and nutrient (nitrogen, phosphorus) accumulation in river-dominated tidal marshes, Georgia, USA. Soil Sci. Soc. Am. J. 74, 1028–1036.
Mackay, D., Callcott, D., 1998. Partitioning and physical chemical properties of PAHs. In: Neilson, A.H. (Ed.), PAHs and Related Compounds: Chemistry. Springer Berlin Heidelberg, pp. 325–345. http://dx.doi.org/10.1007/978-3-540-49697-7_8.
Martins, M., Ferreira, A.M., Vale, C., 2008. The influence of Sarcocornia fruticosa on retention of PAHs in salt marsh sediments (Sado estuary, Portugal). Chemosphere 71, 1599–1606.
Mathew, S., et al., 2019. Bull island: characterization and development of a modern barrier island triggered by human activity in Dublin Bay, Ireland. Ir. Geogr. 52, 75–100.
McGovern, E., et al., 2002. Winter nutrient monitoring of the Western Irish Sea – 1990 to 2000.
McLeod, Elizabeth, et al., 2011. A blueprint for blue carbon: toward an improved understanding of the role of vegetated coastal habitats in sequestering CO_2. Front. Ecol. Environ. 552–560. http://dx.doi.org/10.1890/110004, https://esajournals.onlinelibrary.wiley.com/doi/10.1890/110004.
Merrill, J.Z., Cornwell, J.C., 2000. The role of oligohaline marshes in estuarine nutrient cycling. In: Weinstein, M.P., Kreeger, D.A. (Eds.), Concepts and Controversies in Tidal Marsh Ecology. Springer Netherlands, pp. 425–441.
Meyers, P.A., 1997. Organic geochemical proxies of paleoceanographic, paleolimnologic, and paleoclimatic processes. Org. Geochem. 27, 213–250.
Murphy, B.T., et al., 2016. The occurrence of PAHs and faecal sterols in Dublin Bay and their influence on sedimentary microbial communities. Mar. Pollut. Bull. 106, 215–224.
Narayan, S., et al., 2017. The value of coastal wetlands for flood damage reduction in the northeastern USA. Sci. Rep. 7, 9463.
Nieder, R., Benbi, D.K., Scherer, H.W., 2011. Fixation and defixation of ammonium in soils: A review. Biol. Fertil. Soils 47, 1–14.
Nixon, S.W., 1980. Between coastal marshes and coastal waters — A review of twenty years of speculation and research on the role of salt marshes in estuarine productivity and water chemistry. In: Hamilton, P., Macdonald, K.B. (Eds.), Estuarine and Wetland Processes: With Emphasis on Modeling. Springer US, pp. 437–525. http://dx.doi.org/10.1007/978-1-4757-5177-2_20.
O'Higgins, T.G., Wilson, J.G., 2005. Impact of the river Liffey discharge on nutrient and chlorophyll concentrations in the Liffey estuary and Dublin Bay (Irish Sea). Estuar. Coast. Shelf Sci. 64, 323–334.
O'Reilly, H., Pantin, G., 1956. Some observations on the salt marsh formation in Co. Dublin. Proc. R. Ir. Acad. B 58, 89–128.
Oros, D., Ross, J., 2004a. Polycyclic aromatic hydrocarbons in San Francisco Estuary sediments. Mar. Chem. 86, 169–184.
O'Sullivan, K., 2019. EPA Investigating Sewage Discharge Into Dublin Bay. The Irish Times, https://www.irishtimes.com/news/environment/epa-investigating-sewage-discharge-into-dublin-bay-1.3807144.
Ouyang, X., Lee, S.Y., 2014. Updated estimates of carbon accumulation rates in coastal marsh sediments. Biogeosciences 11, 5057–5071.
Radabaugh, K., Powell, C., Bociu, I., Clark, B., Moyer, R., 2016. Plant size metrics and organic carbon content of Florida salt marsh vegetation. Wetl. Ecol. Manag. 25.
Radu, T., Diamond, D., 2009. Comparison of soil pollution concentrations determined using AAS and portable XRF techniques. J. Hazard. Mater. 171, 1168–1171.
Radu, T., et al., 2013. Portable X-ray fluorescence as a rapid technique for surveying elemental distributions in soil. Spectrosc. Lett. 46, 516–526.
Renzi, J.J., He, Q., Silliman, B.R., 2019. Harnessing positive species interactions to enhance coastal wetland restoration. Front. Ecol. Evol. 7.
Rogers, K., et al., 2019. Wetland carbon storage controlled by millennial-scale variation in relative sea-level rise. Nature 567, 91–95.
Rumolo, P., Barra, M., Gherardi, S., Marsella, E., Sprovieri, M., 2011. Stable isotopes and C/N ratios in marine sediments as a tool for discriminating anthropogenic impact. J. Environ. Monit. 13, 3399–3408.
Schuerch, M., et al., 2018. Future response of global coastal wetlands to sea-level rise. Nature 561, 231.

National parks & wildlife service. 0000. North Bull Island SPA (004006). https://www.npws.ie/content/publications/north-bull-island-spa-004006-conservation-objectives-supporting-document.
Skerrett, H.E., Holland, C.V., 2000. The occurrence of Cryptosporidium in environmental waters in the greater Dublin area. Water Res. 34, 3755–3760.
Sokol, N.W., Sanderman, J., Bradford, M.A., 2019. Pathways of mineral-associated soil organic matter formation: Integrating the role of plant carbon source, chemistry, and point of entry. Glob. Change Biol. 25, 12–24.
Stevens, L., Olsen, A.R., 1999. Spatially restricted surveys over time for aquatic resources. J. Agric. Biol. Environ. Stat. 4, 415–428.
Stumpner, E.B., et al., 2018. Sediment accretion and carbon storage in constructed wetlands receiving water treated with metal-based coagulants. Ecol. Eng. 111, 176–185.
Sundby, B., Vale, C., Caetano, M., Luther, G.W., 2003. Redox chemistry in the root zone of a salt marsh sediment in the Tagus Estuary, Portugal. Aquat. Geochem. 9, 257–271.
Sutton-Grier, A.E., Sandifer, P.A., 2018. Conservation of wetlands and other coastal ecosystems: a commentary on their value to protect biodiversity, reduce disaster impacts, and promote human health and well-being. Wetlands http://dx.doi.org/10.1007/s13157-018-1039-0.
Tollefson, J., 2018. Climate scientists unlock secrets of 'blue carbon'. Nature http://dx.doi.org/10.1038/d41586-018-00018-4, http://www.nature.com/articles/d41586-018-00018-4.
UNESCO Biosphere Periodic Review Report, 2014. North Bull Island UNESCO Biosphere Periodic Review Report. ResearchGate, https://www.researchgate.net/publication/306012986_North_Bull_Island_UNESCO_Biosphere_Periodic_Review_Report_2014.
Vane, C., Harrison, I., Kim, A., 2007. Polycyclic aromatic hydrocarbons (PAHs) and polychlorinated biphenyls (PCBs) in sediments from the Mersey Estuary. U.K. Sci. Total Environ. 374, 112–126.
Verardo, D.J., Froelich, P.N., McIntyre, A., 1990. Determination of organic carbon and nitrogen in marine sediments using the Carlo Erba NA-1500 analyzer. DSRA 37, 157–165.
Vestin, K., 2001. The Seville Strategy for Biosphere Reserves, Vol. 13. https://unesdoc.unesco.org/ark:/48223/pf0000123605.
Vymazal, J., 2007. Removal of nutrients in various types of constructed wetlands. Sci. Total Environ. 380, 48–65.
Vymazal, J., 2011. Constructed wetlands for wastewater treatment: Five decades of experience †. Environ. Sci. Technol. 45, 61–69.
Walker, T.R., MacAskill, D., Rushton, T., Thalheimer, A., Weaver, P., 2013. Monitoring effects of remediation on natural sediment recovery in Sydney Harbour, Nova Scotia. Environ. Monit. Assess. 185, 8089–8107.
Wilson, J.G., 2005. Diffuse inputs of nutrients to Dublin Bay. Water Sci. Technol. 51, 231–237.
Wilson, J.G., Allott, N., Bailey, F., Gray, N., 1986. A survey of the pollution status of the Liffey estuary, 3, 1986, p15-20 Journal Article, 1986. Ir. J. Environ. Sci. 3, 15–20.
Wilson, J.G., Brennan, M., Murray, A., 2002. Particulate inputs to Dublin Bay and to the South Lagoon, Bull Island. Hydrobiologia 475, 195–204.
Wilson, J.G., Forrest, N., 2005. Population dynamics, biomass and productivity of Limapontia depressa (Gastropoda, Opisthobranchia) at Bull Island, Dublin, Ireland. Aquat. Ecol. 38, 575–585.
Wilson, J.G., Parkes, A., 1998. Network analysis of the energy flow through the Dublin Bay ecosystem. Biol. Environ. Proc. R. Ir. Acad. 98B, 179–190.
Yunker, M.B., et al., 2002. PAHs in the Fraser River basin: a critical appraisal of PAH ratios as indicators of PAH source and composition. 33. pp. 489–515.
Zhang, C., et al., 2014. Effects of sediment geochemical properties on heavy metal bioavailability. Environ. Int. 73, 270–281.